J. Fluid Mech. (1999), *vol.* 399, *pp.* 355–376. Printed in the United Kingdom

Experimental investigation of the global instability of plane sheet flows

By LUIGI DE LUCA

Università di Napoli 'Federico II' – DETEC, P. le Tecchio, 80, Naples 80125, Italy

(Received 10 March 1999 and in revised form 26 June 1999)

A *global* stability investigation of two-dimensional vertical liquid sheet flows is experimentally carried out. The motivation is that previous investigations addressed the study of the *local* absolute/convective character of such flows, thus they are not able to predict the actual critical flow Weber number corresponding to sheet rupture. The objective of the paper is twofold: first, the link between local absolute and global instabilities is investigated and the measured length of the absolute instability region is correlated with the non-parallelism parameter (sheet slenderness ratio which is the reciprocal of the Froude number); then, a criterion to predict the flow Weber number value at sheet rupture is given for which the critical Weber number is correlated with Froude and Reynolds numbers. Tests are carried out on liquid (low-concentration water solutions of surfactants and low-viscosity motor oil) sheets issuing from a nozzle with a long horizontal exit section in still air under the gravitational field. A major goal of the experiments is the determination of the vertical location where the local Weber number equals unity, because this yields the length of the absolute instability region. This location is determined by observing the standing sinuous waves generated by an obstacle placed normally to the sheet, and by measuring the angle between the tangent to the wave at the obstacle and the vertical direction for the minimum liquid flow rate necessary to maintain the sheet stable (global instability onset).

1. Introduction

Two-dimensional plane jets falling freely under the effect of gravity (liquid sheet flows) are employed in many industrial applications, which include coating processes and environment protection in chemical and/or nuclear technology (where sheet annular configurations are also considered). Such applications are well summarized in the paper by Finnicum, Weinstein & Ruschak (1993), whereas Chubb *et al.* (1994) investigated the sheet flows as low-mass radiating surfaces for Space application. In a more recent paper Söderberg & Alfredsson (1998) developed a study aimed towards the paper industry, where a fibre suspension is formed into a plane liquid jet by a nozzle.

Owing to its increased industrial importance, starting from the fifties research has been focused on the dynamics and the instability (leading to break-up or rupture) of the liquid sheets. A quick review of the basic literature follows, starting from the experimental observations. Brown (1961) studied the behaviour of a plane liquid jet (curtain) impinging on a moving surface. He found the minimum liquid flow rate to maintain a stable sheet by observing that equilibrium must be maintained at a free edge between the inertia forces and the surface tension. When a free edge appears because of the formation of a hole, such a hole does not grow if the oncoming

momentum flux is greater than the surface tension force; otherwise it grows and the curtain disintegrates. His pioneering physical interpretation remains a milestone for modern theoretical and numerical investigations. Later, as some authors tried to explain the disagreement between experimental data and results coming from the temporal mode analysis, Crapper, Dombrowski & Pyott (1975) observed that if photographs were taken at different times, the wave amplitude was unchanged at the same distance from the nozzle exit section, thus giving rise to the spatial mode analysis devoted to this kind of flow. On the other hand, Carlomagno (1974) extended Lee's (1963) work on the instability of a film coating a two-dimensional cylinder to the case of a continuous downflow from the cylinder. Depending on the flow rate value, different flow regimes were observed: sheets, sheets and discrete vertical jets (or threadlines), jets, drops. Flow regimes qualitatively similar to those mentioned above were found by Pritchard (1986), who studied the free-surface class of flows arising when the fluid is poured over the end of a flat plate into a reservoir below the plate. These regimes were also observed by Limat *et al.* (1992) in an experimental set-up similar to that employed by Lee (1963) and Carlomagno (1974): a horizontal hollow half-cylinder was supplied with liquid that overflowed, ran over the external sides and was collected below the cylinder. More recently de Luca & Meola (1995) analysed the continuous downflow of a liquid from a two-dimensional nozzle and found basically the same class of flows described above together with a phenomenon, the Reynolds ridge, that is a peculiarity of the presence of surfactants in the test liquid. In order to understand the development of free plane jets, Söderberg & Alfredsson (1998) investigated the basic laminar flow and its stability, both numerically and experimentally. The experiments showed that the wave instability results in a break-up of the laminar jet, giving rise to a turbulent jet which appears to contain streaky structures. They visualized the sheet break-up by means of a particle visualization technique and observed that the break-up creates streamwise streaks in the plane jet which are much stronger than streaks originating from the inside of the nozzle.

From the theoretical point of view, Squire (1953) and later Hagerty & Shea (1955) performed an inviscid analysis on a sheet of uniform thickness and found that instability occurs if the Weber number (ratio of inertia forces to liquid surface tension) is greater than unity. Subsequent papers took into account the effects of liquid viscosity. Crapper, Dombrowski & Jepson (1975) demonstrated that viscosity has no effect on the initial stages of wave growth. Lin (1981) asserted that viscosity has the dual roles of increasing both the amplification rate and the damping rate of the disturbances. This result was then confirmed by Lin, Lian & Creighton (1990) who found that, contrary to the case of a round jet (Lin & Lian 1989), the critical Weber number equal to unity is insensitive to the gas-to-liquid density ratio and the Reynolds number. These authors asserted also that the sinuous (or antisymmetric) modes of disturbances are convectively unstable for Weber numbers above the critical one equal to unity, while they are pseudo-absolutely unstable below the critical Weber number (the term pseudo-absolute instability was used to mean that the relevant Green's function is bounded but is non-vanishing for all time and all spatial positions). Li & Tankin (1991) showed that the liquid viscosity introduces an additional temporal mode which destabilizes a certain range of wavenumbers and is referred to as viscosity-enhanced instability. De Luca & Costa (1997*b*), besides some other considerations which will be discussed later, confirmed substantially the major result of Lin *et al.* (1990) but, by employing an inviscid model, found that below the critical Weber the sheet is fully absolutely unstable with algebraic growth of disturbances. In agreement with the experimental evidence, they asserted that the sheet break-up is linked to the

presence of this absolute instability and, following the finding of Crapper *et al.* (1975), they conjectured that the liquid viscosity may act to remove the algebraic growth, but the time after which this occurs could be not sufficient to avoid possible nonlinear phenomena appearing and breaking up the sheet. Teng, Lin & Chen (1997) included the effect of viscosity of the ambient gas and confirmed that the critical Weber number is approximately equal to one and is weakly dependent on the other governing parameters. Söderberg & Alfredsson (1998) carried out a coupled experimental and theoretical stability investigation aimed at studying the influence of the relaxation process of the velocity profile. They considered a parallel flow (i.e. constant sheet thickness) and employed a temporal linear stability analysis.

In summary, the present state of art of the modelling of liquid sheet flow instability addresses the absolute or convective character of the instability and takes into account the non-parallelism of the flow (due to gravity) in an unsatisfactory way. In fact, Lin *et al.* (1990), Teng *et al.* (1997), and de Luca & Costa (1997*b*), all considered a locally non-parallel flow, so that they predict the existence of a critical value of the *local* Weber number equal to unity, but are not able to predict the vertical location where this critical value is attained, i.e. they cannot predict the critical *flow* Weber number. Hence, the flow conditions producing the sheet rupture remain substantially unknown and the need to develop the so-called global instability analysis arises clearly from the above discussion. The concepts of absolute and convective instability in fluid dynamics are now well established (the reader is referred to the exhaustive paper by Huerre & Monkewitz 1990); on the other hand, the link between the local absolute instability and the global instability (producing the basic flow break-up) in non-parallel flows is currently under study. For the case of incompressible two-dimensional shear flow Monkewitz, Huerre & Chomaz (1993) demonstrated that the presence of a region of absolute instability is just a necessary condition for the onset of amplified global oscillations and specified the order of magnitude of the streamwise length of the absolute instability region in order for global resonances to occur. All these ideas will be reviewed in the next section, especially as far as the liquid sheet flows are concerned.

The present work draws its motivation from the above discussion and is aimed to give a prediction criterion for the sheet rupture; in other words, a global instability analysis is carried out that is aimed at determining the critical flow Weber number corresponding to the break-up. The global linear stability analysis of falling capillary round jets has already been developed by Le Dizès (1997), who found that the global instability is caused by a region of local absolute instability located near the nozzle. Yakubenko (1997) studied the inclined round jet for which no region of absolute instability is found, i.e. the flow is locally convectively unstable at every streamwise location. To the knowledge of the present author no global instability theory has been developed for plane liquid sheet flows. Since the major weakness in the past studies, which included various kinds of flows, is the lack of experimental validation of the different theoretical developments, the contribution of the present investigation is that the global stability analysis of plane sheet flows is performed experimentally. The objective is twofold: first, the link between local absolute and global instabilities is investigated and the measured length of the absolute instability region is correlated to the non-parallelism parameter (for the present flow the sheet slenderness ratio that may be interpreted as the reciprocal of a Froude number); then, a criterion to predict the flow Weber number value of sheet rupture is given, for which the critical Weber number is correlated to the Froude and Reynolds numbers.

The paper is organized as follows. Section 2 gives the theoretical background of the concepts of local and global instabilities, as well as their application to plane liquid

sheet flows. Section 2 also examines some characteristics of the basic laminar sheet flow and of the wave patterns developing on it. Finally, it defines the objectives of the present experimental investigation. The experimental set-up and testing procedure are described in § 3 and the results are discussed in § 4. Section 5 summarizes the main conclusions.

2. Theoretical outline

This section is devoted to a summary of the theoretical background of the concepts of local and global instability, as well as their application to plane sheet flows. Some other physical considerations about the base laminar flow and the wave propagation on the sheet interface will be also reported, together with the objective of the present experiments and their design.

2.1. *Absolute/convective and local/global instabilities*

One of the major modern topics in the field of fluid dynamic instability is understanding the link between local and global instability of non-parallel flows. It is known that the concept of absolute and convective instability applies in principle only to parallel flows, i.e. to flows invariant under continuous translations in the streamwise direction. In physical terms, an absolutely unstable flow behaves as an oscillator, i.e. it only needs a small impulse to develop time-growing oscillations at any fixed location. The response of the system is intrinsic and independent of the initial impulse. A convectively unstable flow behaves as a spatial amplifier of extrinsic noise and ultimately returns to the undisturbed state if the external excitation is turned off (Bers 1975; Huerre & Monkewitz 1990).

Many actual flows are not parallel. For these, if the base flow develops slowly in the streamwise direction the classification of the instability as absolute or convective is still valid, but only in a *local* sense. However, since in particular the local absolute instability refers to a fictitious parallel mean flow, it cannot in general be experimentally observed in a spatially developing flow and only the *global* properties are meaningful, where following Huerre & Monkewitz (1990) the term *global* is used to mean that the flow is stable or unstable with respect to infinitesimal fluctuations in the entire flow field. A crucial point is to relate the local flow properties established theoretically to the observed global behaviour of a non-parallel flow (the nonlinear effects of the global instability are indeed observed in most laboratory experiments). This question has been approached by Chomaz, Huerre & Redekopp (1988) under the assumption that the base flow develops slowly in the streamwise direction (on the scale of the instability wavelength). By using a model based on the Ginzburg–Landau equation, some characteristics of global modes and their relation to local convective and absolute instabilities have been illustrated. The basic finding (see also, among others, Monkewitz 1990) is that local absolute instability may lead to global instability, but the region of the absolute instability needs to be sufficiently long; conversely, convective instability corresponds to global stability, if boundary and long-range feedback effects are negligible. Monkewitz (1988) showed that the sequence of transitions in the wake of a cylinder, as the Reynolds number is raised, does indeed follow the sequence of transitions in the model problem of Chomaz *et al.* (1988). Starting from the early paper of Mathis, Provansal & Boyer (1984), several authors (referenced in Huerre & Monkewitz 1990) identified the supercritical Hopf bifurcation to a global mode and its final nonlinear saturation in the form of self-sustained oscillations commonly referred to as the von Kármán vortex street.

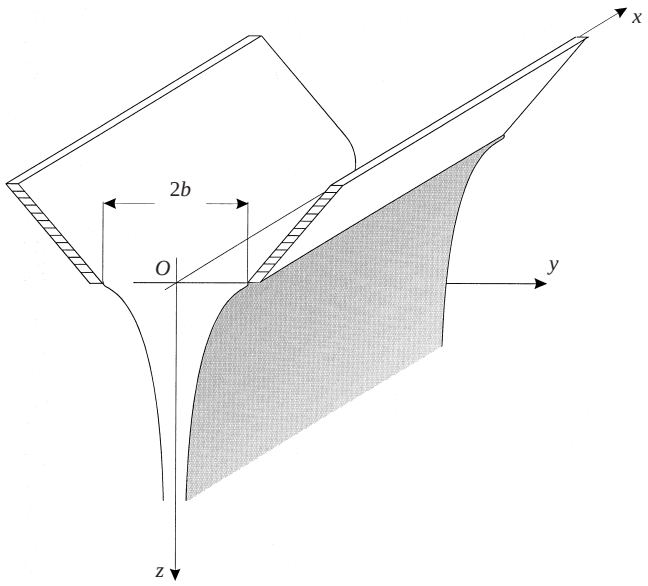

FIGURE 1. Liquid sheet flow under gravity.

Monkewitz *et al.* (1993) gave a more precise specification of the streamwise length of absolute instability that is necessary before global modes become amplified: for the semi-infinite flow domain global instability results whenever the interval of absolute instability adjacent to the boundary grows as $\Delta Z = O(\varepsilon^{2/3})$, Z being the dimensionless slow streamwise spatial coordinate and ε the parameter characterizing the degree of spatial inhomogeneity (or non-parallelism) of the basic flow. It is worth pointing out that this result refers to an incompressible two-dimensional shear flow investigated under the assumption that the far-field pressure feedback between distant points in the field is negligible. In the absence of body forces, the ε parameter is related to the flow Reynolds number Re by $\varepsilon = O(Re^{-1})$. Le Dizès (1997) proved the falling capillary round jet to be globally unstable above the local absolute/convective transition, in qualitative agreement with the conjecture made previously by Monkewitz (1990) that the global transition may correspond to the transition to the dripping regime of vertical round jets. Furthermore, the region of absolute instability necessary for global instability, of $O(\varepsilon^{1/2})$, in this case ε being linked to the Froude number, is found to be larger than $O(\varepsilon^{2/3})$ found for the semi-infinite shear flow.

2.2. *Character of the instability of plane sheet flows*

The main previous results concerned with the instability of liquid sheet flows have been reviewed in the introduction section. Here it is also recalled that Lin (1981), who employed a spatial modes approach, stated the sheet to be temporally stable but spatially unstable for Weber number less than unity, namely for disturbances whose group velocity is directed upstream. The pseudo-absolute instability found by Lin *et al.* (1990) and the local absolute instability algebraic growth with time found in the inviscid case by de Luca & Costa (1997*b*) have been already discussed.

It is worth pointing out that, contrary to previous papers, these last authors took into account the gravity effects by introducing a slow scale for the vertical length, and this allowed them to consider the flow as quasi-parallel or locally parallel. The

sheet slenderness ratio

$$\varepsilon = b/S, \tag{1}$$

where b is the half-width of the nozzle and

$$S = w_0^2/2g, \tag{2}$$

is the typical vertical length scale (w_0 is the mean velocity at the nozzle exit section and g is the gravity acceleration), was introduced as a small parameter relating the slow spatial coordinate Z to the fast one z. If z^* is the dimensional vertical spatial coordinate, then $z = z^*/b$, $Z = z^*/S$, and $Z = \varepsilon z$. The adopted Cartesian coordinate system (x, y, z), x and y denoting the axial and lateral coordinates made dimensionless with respect to b, is shown in figure 1. The problem was solved by means of the multiple scale method, ε characterizing the degree of non-parallelism of the flow. Introducing the flow Froude number, $Fr = w_0^2/2gb$, it is $\varepsilon = 1/Fr$. For sinuous anti-symmetric disturbances (displacing each of the free surfaces in the same direction) a basic result was that a critical streamwise location Z_{cr}, where the local Weber number equals unity, separates a region of local absolute instability (which is present upstream of Z_{cr} and therefore downstream of the nozzle from which the sheet originates) from a region of local convective instability. The *local* Weber number is defined as

$$We_\eta = \frac{\rho w^2 \eta}{\sigma} \tag{3}$$

where w and η are the local sheet velocity and half-thickness, respectively, ρ is the liquid density and σ its surface tension. If the *flow* Weber number is introduced,

$$We = \frac{\rho w_0^2 b}{\sigma} \tag{4}$$

the condition of $We_\eta = 1$ turns out to be $We = \overline{\eta}$, where $\overline{\eta} = \eta/b$ is the dimensionless sheet half-thickness. Thus, the transition from absolute to convective local instability occurs where $We_\eta = 1$ or, alternatively, where $We = \overline{\eta}$. By introducing the liquid flow rate per unit length $Q = 2w_0 b$, the flow Weber number may be re-written as $We = \rho Q^2/4\sigma b$. It is easy to see that the vertical location Z_{cr} at which the sheet experiences the transition of instability moves downstream as the liquid flow rate is reduced or the surface tension is increased. This finding is depicted in figure 2 where a typical trend of the dimensionless sheet interface profile as a function of the slow coordinate Z is reported. It is clear that if $We_2 < We_1$, then $Z_{cr2} > Z_{cr1}$.

Following the theoretical developments of Chomaz *et al.* (1988), and the finding of Le Dizès (1997), de Luca & Costa (1997*b*) hypothesized that the sheet behaves as a globally unstable system (i.e. it breaks up) only if the region of absolute instability is sufficiently long. This conjecture agrees perfectly with the experimental evidence that the sheet breaks up as the flow rate is reduced (e.g. Brown 1961; de Luca & Meola 1995), all other quantities being kept constant. The local analysis allowed the authors to state that the vertical spatial length of the absolute instability region is determined by the location where the local Weber number equals unity, or equivalently where the flow Weber number equals the dimensionless sheet thickness, but it cannot predict the critical flow Weber number giving the rupture of the sheet. To do this it is necessary to develop a global instability investigation, which is the subject of the present paper. In the opinion of the present author this viewpoint goes beyond the major conclusions of the previous literature, where for instance Teng *et al.* (1997) affirmed that 'the manner in which absolute instability leads to the highly non linear phenomenon of rupture

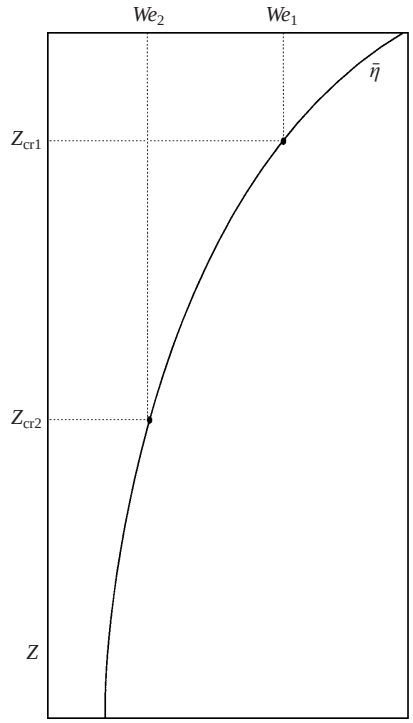

FIGURE 2. Location of local absolute/convective transition along the sheet.

remains unknown', and Söderberg & Alfredsson (1998) concluded that 'in order to fully understand the importance of the different modes of instability it is believed that investigations should be undertaken which include effects of non-parallel flow and the possibility for absolute instability'.

2.3. *Laminar base flow and wave patterns*

In principle, the free falling jet emanating from a nozzle belongs to the so-called die-swell problem, but in the related literature gravity effects were often ignored. Indeed, depending on the relative magnitudes of the gravitational and viscous forces, the influence of the former on the jet shape may be very important (see, among others, Ahn & Ryan 1991). In the limiting case of the absence of gravity the shape of a Newtonian jet emerging from a die or nozzle strongly depends on the Reynolds and capillary numbers: at relatively low Reynolds numbers the jet expands (swelling effect), at high Reynolds the jet contracts, whereas the surface tension has the effect of reducing both swelling and contraction. De Luca & Costa (1995) developed a computational model in which inertia, viscous, gravity and surface tension forces were all taken into account and showed that the inviscid inertia–gravity solution is approached for jet Reynolds numbers greater than 50. Söderberg & Alfredsson (1998) analysed numerically the influence of two shapes of the nozzle from which the jet originates: the plane channel and the slit. While in the case of the channel the jet emanating into an ambient gas (with negligible viscosity and density) relaxes to eventually become uniform, the flow through the slit nozzle is essentially inviscid. A viscous ambient gas also affects the velocity distribution in the jet, and because of this the jet will never be uniform, but it will continue to expand. However, if the viscosity and density of the gas are much lower than those of the liquid, this process

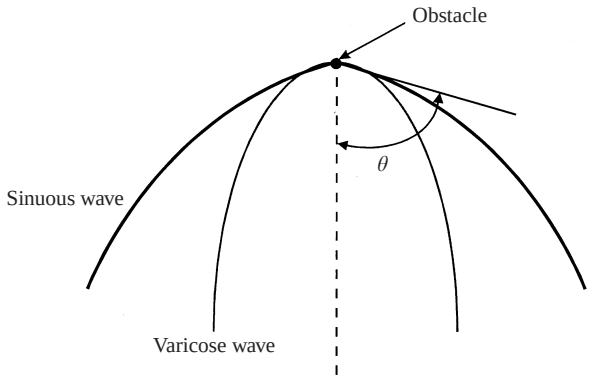

FIGURE 3. Sketch of sinuous and varicose waves produced by an obstacle on the sheet interface.

is very slow. As will be discussed later, the nozzle shape employed in the experiments described in the present paper is of the slit type.

The liquid sheet under gravity behaves as a non-homogeneous, non-isotropic, dispersive and moving medium. It has long been known that two different kinds of waves may develop on thin liquid sheets at any given frequency: sinuous and varicose waves (Taylor 1950). Sinuous waves correspond to anti-symmetric disturbances which displace each of the free surfaces in the same direction. On the other hand, symmetric disturbances which displace the two interfaces in opposite directions give rise to varicose waves. If the wave amplitude is assumed small, the wave-induced mass transport is negligible and the theoretical study of the wave–current interaction can be dealt with by specifying the current in advance. Surface-active agents in the liquid may play an interesting role, as described earlier by Lin & Roberts (1981). These authors also stated that for relatively long wavelengths the wave pattern does not depend on the liquid viscosity.

Since the current is accelerating in the vertical direction, the parameters describing the wave train should change greatly. However, de Luca & Costa (1997*a*) found that if the length scale of the current variations is much longer than a typical wavelength, one may assume that at any given point the waves have the same properties as a plane wave train on a uniform current, and that the parameters describing the wave train, namely wavelength and amplitude, change slowly with the current. The condition under which (relatively long) sinuous waves occur is $We > \overline{\eta}$. The angle θ between the tangent to the curve of constant phase of sinuous waves and the vertical (figure 3) can be predicted to be (Lin & Roberts 1981; Finnicum *et al.* 1993; de Luca & Costa 1997*a*)

$$\theta = \sin^{-1}(1/\sqrt{We_\eta}). \tag{5}$$

De Luca & Costa (1997*a*) also found that the flow acceleration in the vertical direction causes both the wavelength and the amplitude to decrease downward.

2.4. *Objective of the present experiments*

The crucial part of the present work is the determination of the (vertical) location adjacent to the nozzle exit section where the local Weber number equals unity, $We_\eta = 1$, because this yields the extent of the absolute instability region. Such a location is determined experimentally by observing the standing sinuous waves generated by an obstacle (a stainless steel rod) placed normally to the sheet. Since the obstacle creates sinuous waves having an angle θ between the tangent to the wave and

the vertical given by (5), at the location sought it forms standing waves developing locally horizontally ($\theta = 90°$). Thus, the location Z_{cr} where $We_\eta = 1$ is determined, for fixed flow conditions (in particular, for a given flow rate), by moving the rod vertically up the sheet until the standing sinuous waves become horizontal. The position of the rod yielding locally horizontal waves for the critical flow rate (minimum value of the flow rate to maintain the sheet stable) finally gives the length ΔZ of the absolute instability region linked to the global instability onset. Within this context it is worth stressing that there is no theoretical connection between stationary waves and absolute instability. The only practical link is that the position of the rod giving locally horizontal sinuous waves at break-up flow rate corresponds to the length of the absolute instability region and thus to the onset of global instability. The wide range of possible flow regimes observed by varying the liquid flow rate has been summarized in the Introduction, where a quick review of previous experimental observations has been reported. For the present experiments the flow is considered stable when a two-dimensional (i.e. the liquid adheres perfectly to the lateral plates of the experimental set-up, as explained in detail in the next section) regular laminar (i.e. no ripples or streaks are present on the liquid–air interface) liquid sheet can be observed. At a certain critical flow rate it is no longer possible to maintain this flow regime, but either ripples (sometimes more or less regular streaks) appear on the interface, which may produce liquid detachment from the lateral plates (as observed in the case of tests carried out with aqueous solutions of surfactants), or a sudden occurrence of discrete vertical jets (sometimes mixed with a restricted sheet flow regime, which is the case of the tests carried out with oil) are detected. In both cases at the critical flow rate the sheet is considered unstable and one talks about sheet break-up; within the present context such a break-up is considered to correspond to the onset of the global instability.

The present testing procedure used to localize the vertical position where $We_\eta = 1$ has already been employed by Finnicum *et al.* (1993); however, these last authors searched this location to determine a singularity point in the sheet profile. In the present paper, on the other hand, the aim is to determine the transition from local absolute to convective instability or, in other words, to measure the extent of the region of the absolute instability for two-dimensional liquid sheets.

That the region of absolute instability has to reach a critical size for the onset of global instability may be subject to criticism, because one might suspect that the presence of only a local absolute instability is sufficient to make the flow break up. This paper is the first experimental confirmation of such a contention within the framework of liquid sheet flows.

3. Experimental set-up and testing procedure

The experimental set-up is basically that described in detail by de Luca & Meola (1995) as well as by de Luca & Costa (1997*a*) and is reported in figure 4. The test liquid from a tank goes through a regulating valve, a flow meter, a flexible tube, a stagnation chamber and is spread out by means of a stainless steel nozzle. Two lateral plates, placed at each end of the nozzle, facilitate the formation of the sheet and guarantee the two-dimensionality of the base motion. In effect, gravity tends to contract the bottom of the sheet, giving it a characteristic triangular shape (de Luca & Meola 1995). Particular care is taken to eliminate any vibration source, control the ambient air to be quite still, bleed the stagnation chamber, eliminate impurity from

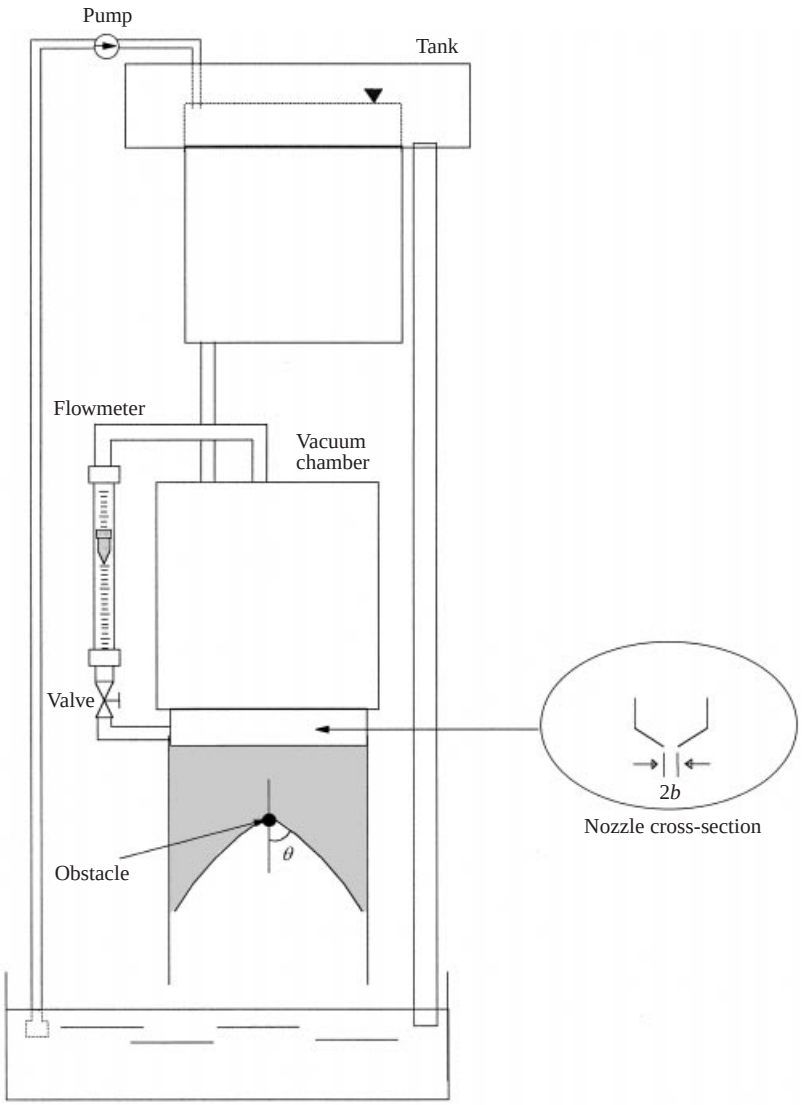

FIGURE 4. Experimental set-up.

the liquid, and ensure the levelling of the nozzle exit section. The liquid is collected in a reservoir below the test section and then pumped back to the tank.

Systematic tests are carried out on liquid sheets issuing from a nozzle with a horizontal exit section, 275 mm long, having five different discharge widths $2b$ ranging from 0.6 to 2 mm. The test liquid consists of either low-concentration aqueous solutions of surfactants (commercial shampoo or soap), or low-viscosity motor oil, whose surface tension σ is 69.0 and 22.1 dyn cm^{-1}, respectively. The nominal (or bulk) surface tension of such solutions is measured by means of a stalagmometer. The liquid density ρ and kinematic viscosity v are also measured; ρ is 0.997 and 0.843 g cm^{-3}, while v is about 1 and 28 cSt for solutions of surfactants and oil, respectively. It would be possible to lower the nominal surface tension of the test liquid by adding to the water an ever-growing amount of surface-active agent (surfactants). However, since

the diffusion time of surfactants towards the liquid–air interface is much greater than the typical descent time of liquid (de Luca & Meola 1995), the surface concentration of surfactants is far from its equilibrium value. In other words, the bulk surface tension of solutions appears practically unchanged when surfactants are added in more quantity to the water.

Figure 4 depicts the detail of the nozzle exit section employed in the present experiments. It is of the slit type and, following Söderberg & Alfredsson (1998), the flow through it is essentially inviscid so that the free interface shape might be estimated to a first approximation by the very simple inviscid inertia–gravity (Torricellian) model

$$\overline{\eta} = \frac{\eta}{b} = \frac{1}{\sqrt{1 + z^*/S}}, \tag{6}$$

with z^* measured from the nozzle exit. However, it is known that relatively close to the nozzle the jet may enlarge (swelling effect), which is not taken into account by the model (6). Recently de Luca & Costa (1995) numerically computed the liquid–air interface profile with inertia, gravity, viscous, and surface tension effects all included. It may be argued that for the sheet flow of water solutions of surfactants analysed (where the Reynolds number based on the average inlet velocity and nozzle half-width, $Re = Q/(2\nu)$, is of the order of 200, the Stokes number, $St = Re/Fr$, ranges from 10 to 150 and the capillary number, $Ca = We/Re$, is of the order of 10^{-3}) equation (6) works quite well outside the so-called extrudate region ($z > 3$). However, within this region the jet contracts more than predicted by the inviscid solution when the surface tension effects are negligible ($Ca = \infty$), but surface tension reduces this contraction and the jet enlarges compared with the shape given by equation (6) for $z < 3$. On the other hand, in the case of tests using oil, the Reynolds number ranges from 2 to 4, St and Ca are of the order of 1 and 10^{-1}, respectively; thus the sheet fully experiences the so-called swelling effect, and the inviscid profile is recovered well outside the extrudate region when surface tension is important. As a consequence, for both aqueous solutions of surfactants and (to a wider extent) oil the vertical location where $We = \overline{\eta}$, given a certain flow Weber number We, moves downstream with respect to the value predicted by equation (6), as illustrated in figure 5. The swelling effect will be taken into account later when the measurements of the extent of the region of absolute instability will be discussed.

For a certain liquid and a fixed nozzle width, experiments generally start with a relatively high value of liquid flow rate per unit length Q so as to prevent the sheet instability. As mentioned in the previous section, a major goal of the present tests is the determination of the (vertical) location adjacent to the nozzle exit section where the local Weber number equals unity, $We_\eta = 1$, or equivalently, in terms of flow Weber number, $We = \overline{\eta}$, because this yields the extent of the absolute instability region. Such a location is determined experimentally by observing the standing sinuous waves generated by an obstacle (a stainless steel rod) placed normally to the sheet. The rod is initially set at a position relatively far from the nozzle (typically 8–10 cm) and is then moved upwards; for each rod position z^* the angle θ of the sinuous waves is measured. Of course, for relatively high liquid flow rates the flow Weber number (namely, the local Weber number at nozzle exit section) is greater than unity and $\theta < 90^\circ$ at $z^* = 0$. Using the regulating valve, the flow rate is decreased and a different angle is obtained for each test condition (Q, z^*). If $We < 1$, locally horizontal waves are detected at a certain z^*_{cr} location, thus confirming that the sheet 'is living' in the presence of an absolute instability. The position of the rod that yields locally

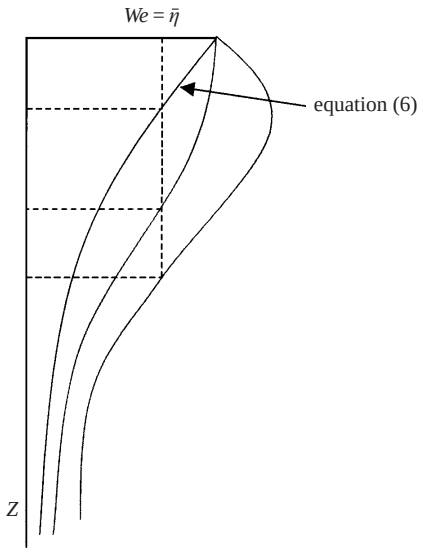

FIGURE 5. Schematic representation of swelling effect.

horizontal waves for the nearly critical flow rate (minimum value of the flow rate to maintain the sheet stable) finally gives the length ΔZ of the absolute instability region as the distance of the rod position from the nozzle exit section. Of course, in practice the value of the measured critical flow rate is a little higher than that corresponding to the instability onset.

The waves are visualized by viewing the sheet plane with a digital video-camera and by illuminating the sheet with lamps to enhance the contrast between crests and troughs. Line scanning frequency is about 16 kHz. The camera is connected to a computer displaying a 512×512 image of the sheet stored for further data post-processing. The wave angle is measured via software on the recorded image by computing the tangent to the sinuous wave at the obstacle. Reproducibility of experimental results is checked both by averaging data taken on a time sequence of images acquired during a certain test session and by repeating the test in a subsequent session. Repeatability of data is very high. Care is taken to maintain the camera lens axis normal to the sheet surface in order to minimize parallax errors. In order to check the influence of the rod diameter on the measurements of the angles, a series of systematic tests is also carried out. It is found that the measured angle is independent of the rod diameter; data presented in this paper refer to a rod diameter of 2 mm.

4. Results

Some typical sinuous wave patterns are shown in figure 6 for oil and in figure 7 for water solution; two different values of nozzle width (0.6 and 2 mm) and rod position z^* (1.5 and 5 cm) are considered (the rod cross-section is clearly recognisable). The images of oil depict very clearly the pattern of only one pair of sinuous waves departing from the rod; in general a very weak trace of varicose waves (much more internal than the sinuous ones) is also visible. In agreement with previous experimental findings of Lin & Roberts (1981) and de Luca & Costa (1997*a*), due to the relatively strong viscosity dissipation effect, varicose waves are hardly detected at all. On the other hand, for water solutions sinuous and varicose waves are both visualized: the

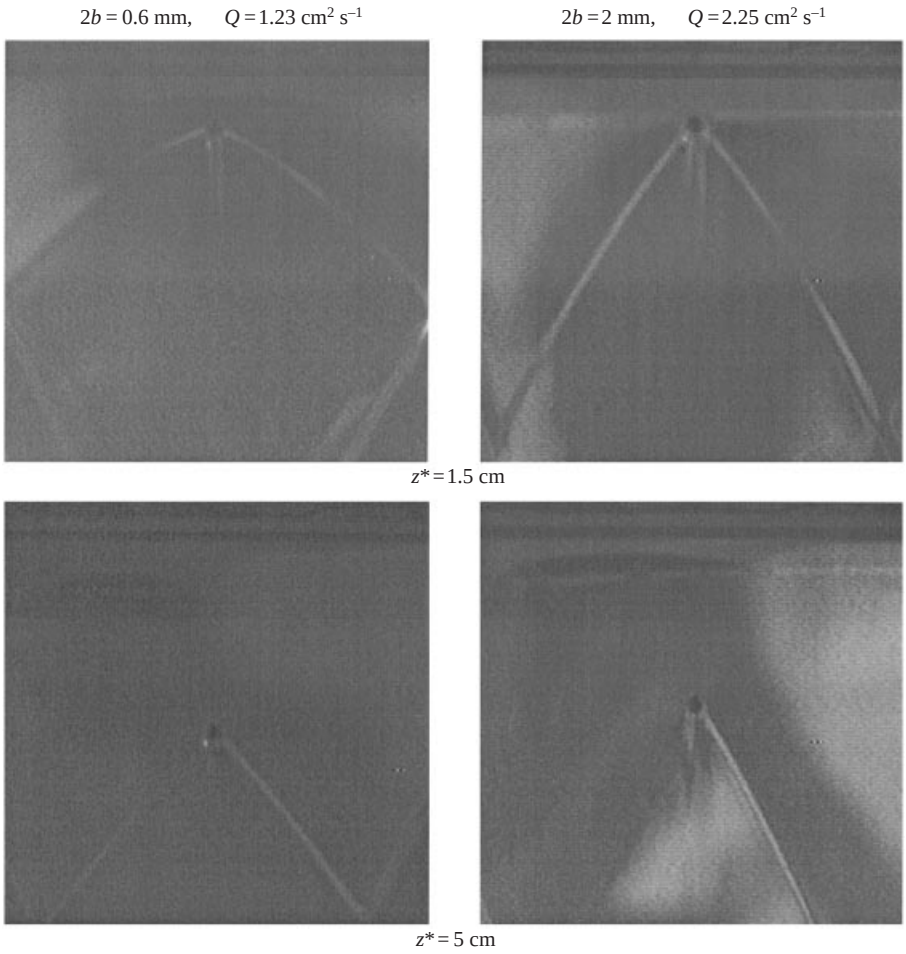

FIGURE 6. Sinuous wave patterns for oil.

sinuous ones, restricted to a very small number of crests, exhibit the typical sharp angle at the obstacle; the varicoses ones are characterized by the classic parabolic shape and show a pattern of a relatively large numbers of crest, the vertex of which protrudes above the rod. For fixed values of nozzle width (and of flow rate per unit length) the images of figures 6 and 7 give a clear indication about the influence of the position of the obstacle upon the angle of standing sinuous waves. The presence of the gravitational field reduces the angle of the sinuous waves at the obstacle when this latter is moved downstream.

In order to assess the accuracy of the measurements of the sinuous wave angles, first a series of tests aimed at investigating the influence of the rod diameter is carried out. During such tests, done for both water solutions and oil, for a fixed value of obstacle diameter, rod position, nozzle width, and liquid flow rate are systematically varied. As an example, for the water solution, the measured values of θ as a function of the rod diameter ϕ are reported in figure 8 for $z^* = 2\,\mathrm{cm}$, $2b = 1.2\,\mathrm{mm}$, $Q = 3.72\,\mathrm{cm}^2\ \mathrm{s}^{-1}$. Data points are scattered around the theoretical value of 46.8° within a 3% spread. In the case of aqueous solutions the wave fan originates just above the obstacle for smaller values of ϕ, which makes measuring the wave angle easier compared with the

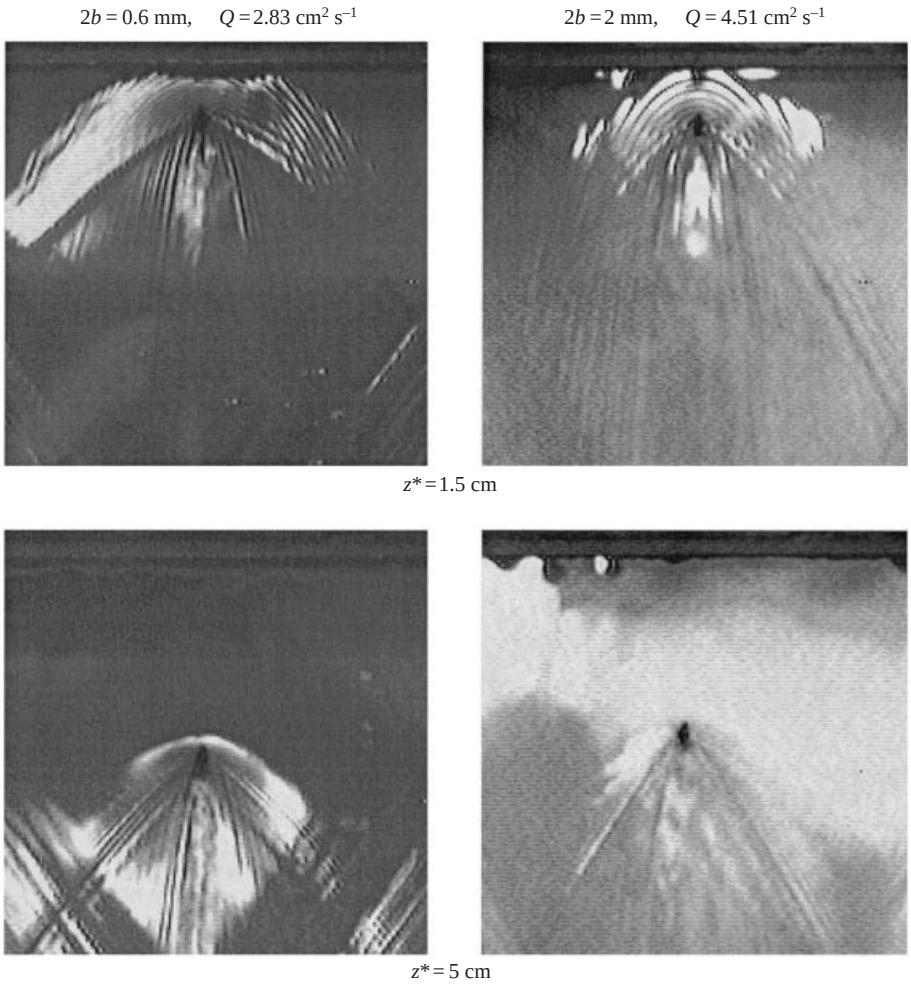

FIGURE 7. Sinuous and varicose wave patterns for water solution.

situation occurring for higher rod diameters for which the waves appear to depart from the rod trace on the recorded image. The upward displacement of the apex of sinuous waves is not noticed during tests with oil. A good compromise value seems to be $\phi = 2\,\text{mm}$, for which all tests are performed.

To localize the vertical position where $We_\eta = 1$, in principle it should be sufficient to record the obstacle position z^*_{cr} giving locally horizontal sinuous waves at the (critical) flow rate of incipient sheet break-up (for each fixed test liquid and nozzle width). However, especially for water solutions, this is not possible in practice because z^*_{cr} is generally very small (less than 5 mm) whilst for rod positions of about 10 mm and less the presence of the varicose waves developing above the obstacle and interfering with the nozzle exit section does not allow a precise visualization of the sinuous waves. Thus, in order to estimate z^*_{cr} at very small z^* values, θ as a function of the position of the rod is extrapolated from curves fitting the measured values. On the other hand, for oil at the smallest values of nozzle width, it is possible to read z^*_{cr} directly on the recorded image, z^*_{cr} being of the order of 10 mm. This is shown on the figure 9 where one may read $z^*_{cr} = 9.15\,\text{mm}$ for $2b = 0.6\,\text{mm}$ and $Q_{cr} = 1.23\,\text{cm}^2\,\text{s}^{-1}$.

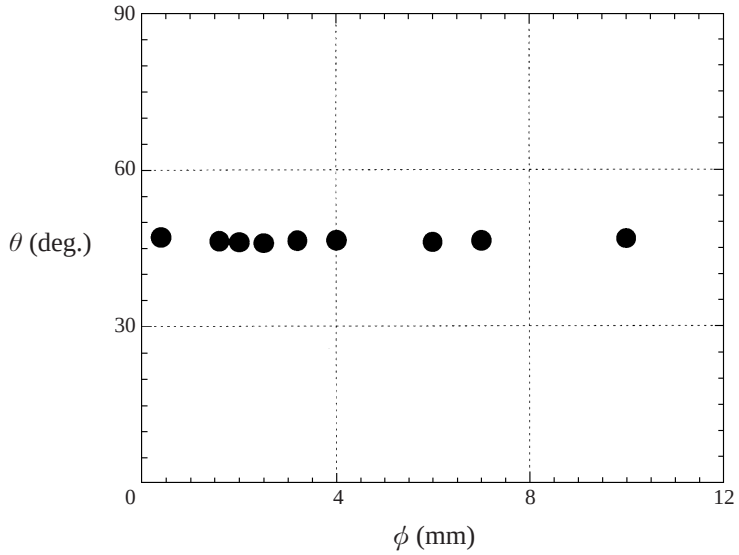

FIGURE 8. Influence of rod diameter on sinuous wave angle: water solution, $2b = 1.2\,\text{mm}$, $z^* = 2\,\text{cm}$, $Q = 3.72\,\text{cm}^2\,\text{s}^{-1}$.

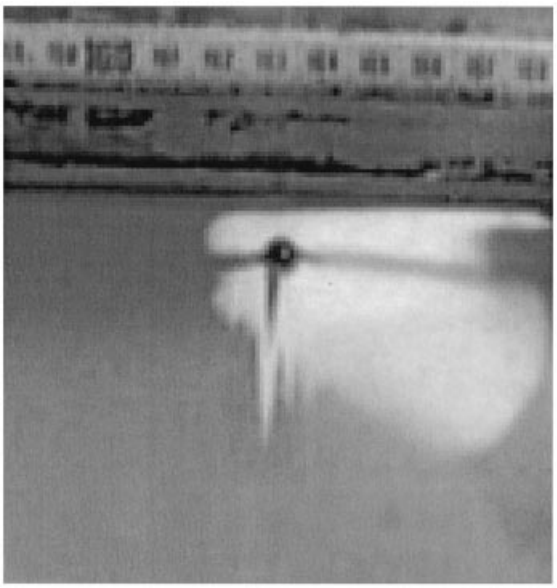

FIGURE 9. Direct experimental determination of locally horizontal sinuous wave for oil: $2b = 0.6\,\text{mm}$, $Q = 1.23\,\text{cm}^2\,\text{s}^{-1}$.

In order to keep data accuracy under control, systematic comparisons are made with the theoretical prediction of equation (5). As an example, experimental versus theoretical θ values are reported in figures 10 and 11, for aqueous solutions and oil, respectively. For the former, liquid data points refer to a fixed nozzle width and various z^* locations of the obstacle and flow rate values, for the latter z^* is fixed while nozzle width and flow rate are varied. Note that in both cases the agreement between theoretical and experimental values is quite good.

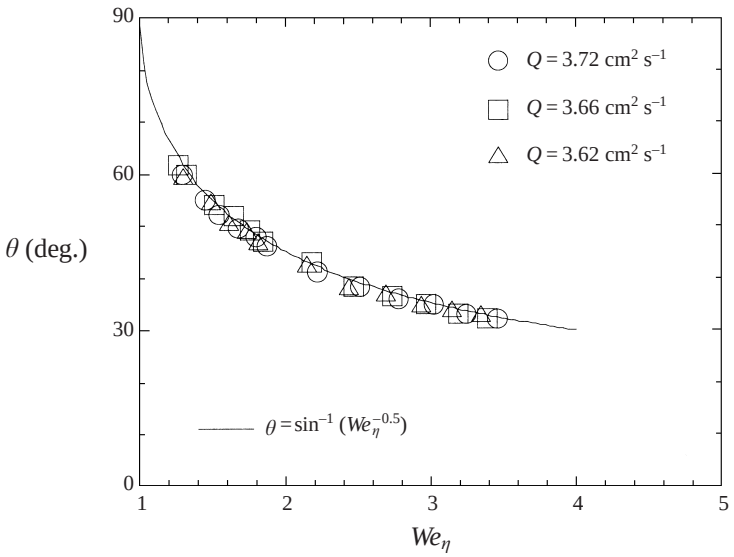

FIGURE 10. Experimental versus theoretical θ angles for water solution; $2b = 1.2\,\text{mm}$.

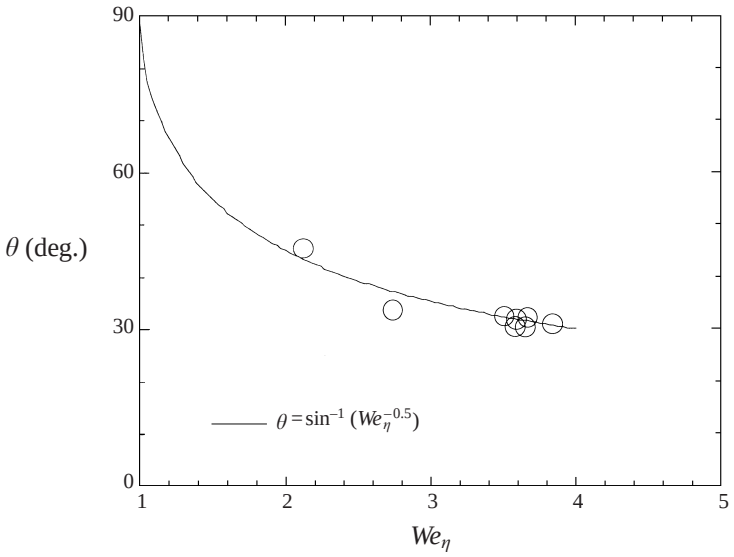

FIGURE 11. Experimental versus theoretical θ angles for oil; $z^* = 3\,\text{cm}$.

Figure 12 depicts a typical determination of z^*_{cr} via data extrapolation, for oil and $2b = 0.6\,\text{mm}$, $Q_{cr} \approx Q = 1.24\,\text{cm}^2\,\text{s}^{-1}$. Extrapolation is numerically computed by means of data fitting based on the law $\theta = \sin^{-1}\left(1/\sqrt{A\sqrt{1+z^*/B}}\right)$, A and B being regarded as fitting parameters to be determined by minimizing the root-mean-square deviation. Note that for the case of figure 12 z^*_{cr} corresponds to the minimum value of the flow rate to maintain the sheet stable, i.e. to the instability (sheet break-up) onset. The test conditions reported in figure 12 are chosen to compare the extrapolation result with the direct measurement of z^*_{cr} as illustrated by figure 9. Such a comparison, when available, seems in general satisfactory.

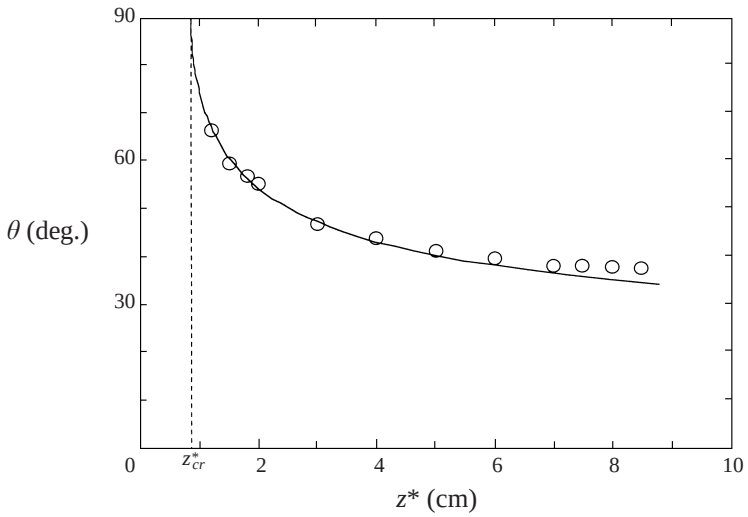

FIGURE 12. Determination of z^*_{cr} via data fitting in the case of oil. Test conditions are the same as in figure 9.

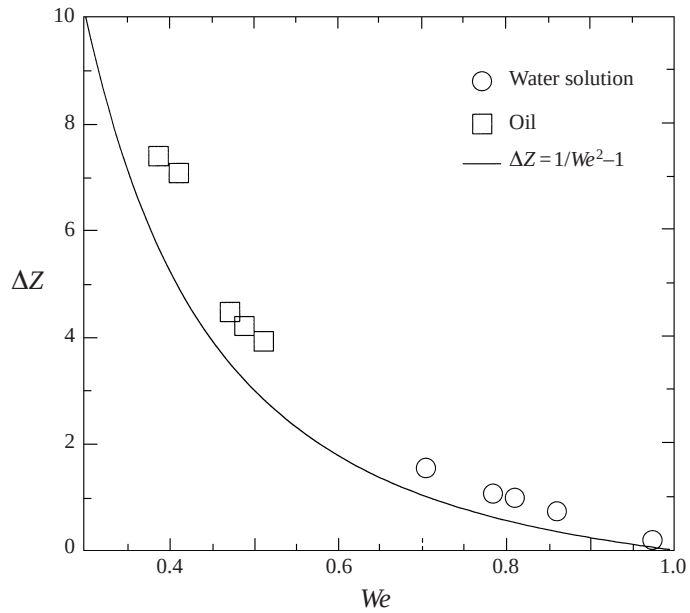

FIGURE 13. Locus of vertical locations of unit local Weber number as a function of flow Weber number.

The locus of dimensionless $Z_{cr} = z^*_{cr}/S$ locations where $We_\eta = 1$ (i.e. $We = \overline{\eta}$), determined either via data extrapolation or directly from images, for both test liquids and the different nozzle width values, is reported in figure 13 as a function of the flow Weber number. Since it is conjectured that such Z_{cr} values represent the length of the absolute instability region at global instability onset, as stated previously, they are denoted by ΔZ in figure 13. In reducing the data, flow Weber number is evaluated as $We = \rho Q^2/(4b\sigma)$ and the slow length scale S as $S = Q^2/(8gb^2)$. Square symbols refer

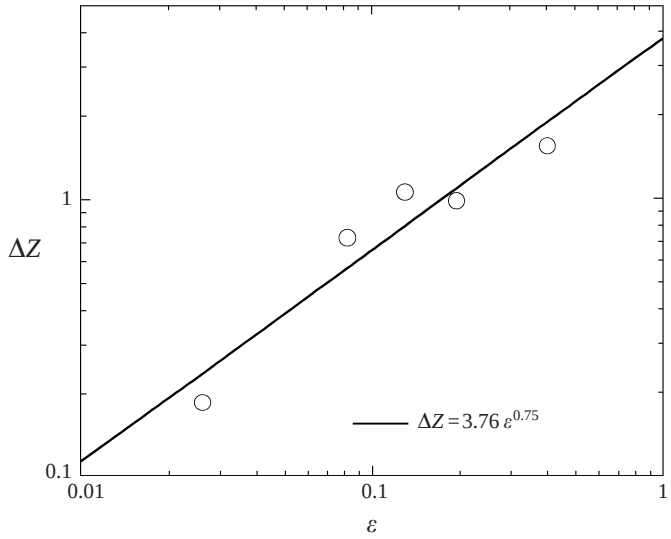

FIGURE 14. Length of the absolute instability region against sheet slenderness ratio, limited to the water solutions tests.

to oil whilst circle symbols refer to water solutions. The continuous line represents the theoretical prediction yielded by the equation

$$\Delta Z = 1/We^2 - 1, \tag{7}$$

which is obtained by assuming that the sheet interface shape may be represented by the very simple inviscid inertia–gravity model of equation (6). Note that if such a model were valid, ΔZ could be evaluated directly from the continuous line of figure 13 by entering the experimental We value evaluated at sheet break-up. Indeed all the experimental data points lie above the curve (7), more so for tests carried out with oil. This occurrence may be explained by the swelling effect experienced by the plane jet relatively close to the nozzle exit, already discussed in § 3 with the aid of figure 5.

Following the theoretical developments of Chomaz *et al.* (1988), based on a rather general Ginzburg–Landau model, Monkewitz *et al.* (1993), relating to a two-dimensional shear flow, and Le Dizès (1997), concerning the falling capillary round jet flow, the dimensionless ΔZ values of figure 13 will be hereafter correlated with the non-parallelism parameter ε. Remember that for the present problem the ε parameter has been defined in § 2.2 as $\varepsilon = b/S$, namely $\varepsilon = 2gb/w_0^2$, and so it may be interpreted as the reciprocal of the Froude number, $\varepsilon = 1/Fr$. In reducing the experimental data ε is evaluated as $\varepsilon = 8gb^3/Q^2$. Figure 14 reports such a correlation of ΔZ with ε restricted to aqueous solution data points only; since for this test liquid the flow Reynolds number based on the sheet half-thickness, $Re = Q/(2\nu)$ is of the order of 200, the flow regime may be considered practically inviscid and a dependence of ΔZ on ε alone is expected (Le Dizès 1997). The equation of the correlation curve which fits present measurements is (full line)

$$\Delta Z = 3.76\,\varepsilon^{0.75}. \tag{8}$$

Note that the region of absolute instability necessary for global instability of plane liquid sheets appears, in its inviscid limit, to be smaller than in the other studies: compare $O(\varepsilon^{0.75})$ with $O(\varepsilon^{2/3})$ which is the result of Monkewitz *et al.* (1993), and $O(\varepsilon^{1/2})$

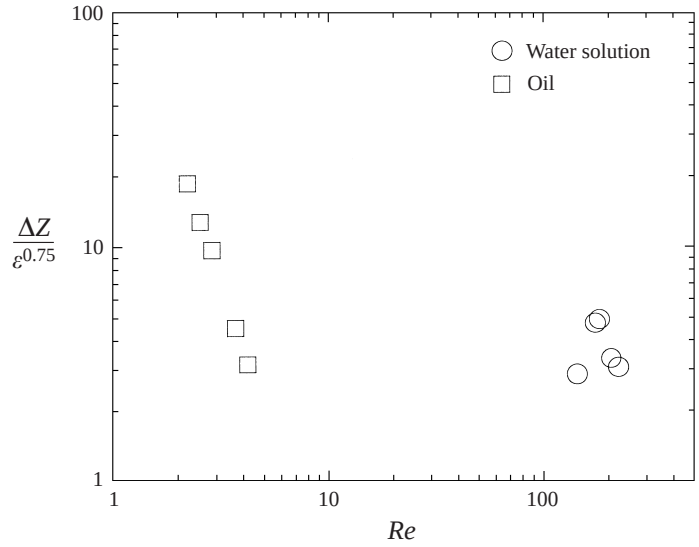

FIGURE 15. Correlation of the length of the absolute instability region with sheet slenderness ratio and Reynolds number.

which was obtained by Le Dizès (1997). This last author proved theoretically that the global modes are composed of three local plane waves interacting at the so-called turning point; the spatial structure of the global modes is prescribed at leading order by the local dispersion relation that defines the local stability properties. The (three) spatial branches of the local dispersion relation give the corresponding wavenumbers of the local plane waves approximating the global mode in the case of round capillary jet. For weakly non-parallel shear flows Monkewitz *et al.* (1993) found that two local plane waves interact at the turning point giving rise to a global mode, because for this class of flows the local dispersion relation is particularly simple and reduces to a single temporal branch with two spatial branches. Thus, in other words, the global dynamics is governed by a Ginzburg–Landau type equation in the direction of propagation of the local waves. For both the flows analysed above the quantities characterizing the global modes (such as global growth rate, critical value of the governing parameter for global transition, length of the region of absolute instability) are correlated with the non-parallelism parameter by a power function of ε whose exponent is strictly linked to the structure of the relevant dispersion relation. Of course, a theoretical confirmation of the present experimental results for a two-dimensional liquid sheet flow will require the development of a global stability analysis for this class of flows.

Following Le Dizès (1997), figure 15 depicts the correlation of ΔZ with both Fr (namely ε) and Re for all experimental data. Those referring to oil, for which sheet break-up Re ranges approximately from 2 to 4, show a marked decreasing trend; a nearly constant (inviscid) asymptotic trend is approached by data points of the water solution. Note that the exponent 0.75 determined by the fitting of figure 14 is employed in the present correlation.

Figure 16 reports the final correlation of the three control parameters, We, ε, and Re, evaluated at the flow rate of sheet break-up, i.e. as conjectured in the present paper at the onset of global instability, for the two test liquids and the different nozzle widths. Since the unitary value of We may be interpreted as the threshold value for the

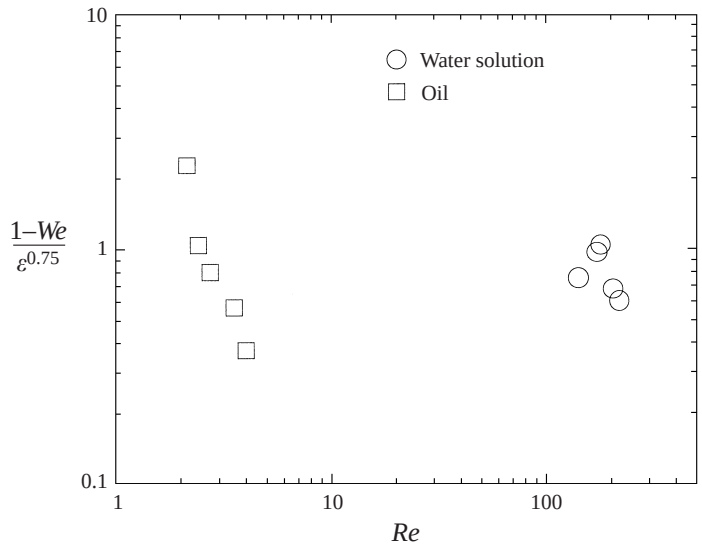

FIGURE 16. Correlation of the three control parameters We, ε and Re evaluated at flow rate of sheet break up (global instability onset).

local absolute/convective transition at the nozzle exit, the quantity $1 - We$ represents how much the critical Weber for the global transition is below the critical Weber for the absolute/convective transition. Figure 16 is a synthesis of the experimental global instability analysis as developed in § 2.2 and may be used to predict the break-up flow Weber number as a function of Froude and Reynolds numbers. As found in figure 15, data for oil exhibit a marked decreasing trend, while those for water solutions seem to approach a nearly constant inviscid asymptotic limit. For the present case of plane liquid sheets the two critical Weber numbers differ by a factor of the order of $\varepsilon^{0.75}$, while for the round vertical jet Le Dizès (1997) found a factor of the order of $\varepsilon^{0.5}$.

5. Conclusions

The *global* stability of two-dimensional vertical liquid sheet flows is experimentally investigated. The work is motivated by the fact that previous investigations addressed the study of the *local* absolute/convective character of such flows, namely they yield the critical local Weber number for the absolute/convective transition but are not able to predict the actual critical Weber number corresponding to the sheet rupture. Following previous theoretical findings on the local stability of plane liquid sheets and an analogous theoretical investigation concerned with the case of vertical round jets, three control parameters are considered: Weber, Froude and Reynolds numbers. The reciprocal of the Froude number is also employed as measure of the degree of non-parallelism of the flow and may be regarded as the sheet slenderness ratio.

Experimental tests are performed on two test liquids: water solutions of surfactants and oil. For each liquid five values of the width of the nozzle exit section, from which the sheet issues, are considered and for each test condition the break-up liquid flow rate is measured. First, in order to investigate the link between local absolute and global instability properties, the length of the absolute instability region is measured. Tests are carried out on liquid sheets issuing from a nozzle with a long horizontal exit section in still air under the gravitational field. The key part is the determination of

the vertical location where the local Weber number equals unity, because this yields the extent of the absolute instability region. This location is determined by observing the standing sinuous waves generated by an obstacle (namely a rod) placed normally to the sheet, and by measuring the angle between the tangent to the wave at the obstacle and the vertical direction. Transition from absolute to convective instability occurs along the sheet at the vertical location where the flow Weber number equals the dimensionless sheet half-thickness. Here the angle between the tangent to the wave at the obstacle and the vertical is 90°. The extent of the absolute instability region is given by this location at the onset of instability, i.e. for the minimum value of liquid flow rate to maintain the sheet stable.

A first qualitative result is that the sheet 'can live' in the presence of a region of absolute instability. Thus an experimental confirmation of the basic theoretical finding of Chomaz *et al.* (1988) is given, namely that self-sustained resonances (global instability) may appear when the system exhibits a region of local absolute instability which is sufficiently large. Remember that these authors refer to a quite different framework, that of an incompressible two-dimensional non-parallel shear flow.

For tests with water solutions it is found that the dimensionless absolute instability interval increases with increasing sheet slenderness ratio as $\varepsilon^{0.75}$. The Reynolds number is of the order of 200 and results obtained with water solutions may be assumed as the asymptotic inviscid limit. Data points for oil, for which sheet break-up Re ranges approximately from 2 to 4, on the other hand show a marked decreasing trend. Note that the region of absolute instability necessary for global instability of plane liquid sheets appears, in its inviscid limit, to be smaller than in the other studies: compare $O(\varepsilon^{0.75})$ with $O(\varepsilon^{2/3})$ which is the result of Monkewitz *et al.* (1993), and $O(\varepsilon^{1/2})$ which was obtained by Le Dizès (1993). This could be related to the order of the pinch-type singularity exhibited by the relevant dispersion relation.

The *experimental global instability analysis* is synthesized in a plot where the break-up flow Weber number (i.e. We evaluated for the minimum flow rate to maintain the sheet stable) is correlated to Froude and Reynolds numbers. Again, data for oil exhibit a marked decreasing trend of $(1-We)/\varepsilon^{0.75}$ as a function of Re, while those for water solutions seem to approach a nearly constant inviscid asymptotic limit. Thus, for the present case of plane liquid sheets the critical Weber for absolute/convective instability (equal to unity) and the critical Weber for global transition differ by a factor of the order of $\varepsilon^{0.75}$, while for the round vertical jet Le Dizès (1997) found a factor of the order of $\varepsilon^{0.5}$.

A theoretical model investigating the global stability behaviour of vertical plane sheet flows is currently under study and will be the subject of a subsequent paper, where nonlinear effects will also be analysed.

The technical assistance of Dr Carosena Meola in designing the experimental set-up and of Carmen Bosso and Andrea Bianco in performing the experimental tests is gratefully acknowledged.

REFERENCES

Ahn, Y. C. & Ryan, M. E. 1991 A finite difference analysis of the extrudate swell problem. *Intl J. Numer. Meth. Fluids* **13**, 1289–1310.

Bers, A. 1975 Linear waves and instabilities. In *Physique des Plasmas* (ed. C. De Witt & J. Peyraud). Gordon & Breach.

Brown, D. R. 1961 A study of the behaviour of a thin sheet of moving liquid. *J. Fluid Mech.* **10**, 297–305.

Carlomagno, G. M. 1974 Moto di un film liquido su un cilindro orizzontale posto in aria calma. *Proc. II Congr. Naz. AIMETA*, IV, pp. 253–262.

Chomaz, J. M., Huerre, P. & Redekopp, L. G. 1988 Bifurcations to local and global modes in spatially developing flows. *Phys. Rev. Lett.* **60**, 25–28.

Chubb, D. L., Calfo, F. D., McConley, M. W., McMaster, M. S. & Afjeh, A. A. 1994 Geometry of thin liquid sheet flows. *AIAA J.* **32**, 1325–1328.

Crapper, G. D., Dombrowski, N. & Jepson, W. P. 1975 Wave growth on thin sheets of non-Newtonian liquids. *Proc. R. Soc. Lond.* A **342**, 225–236.

Crapper, G. D., Dombrowski, N. & Pyott, A. D. 1975 Large amplitude Kelvin-Helmholtz waves on thin liquid sheets. *Proc. R. Soc. Lond.* A **342**, 209–224.

Finnicum, D. S., Weinstein, S. J. & Ruschak, K. J. 1993 The effect of applied pressure on the shape of a two-dimensional liquid curtain falling under the influence of gravity. *J. Fluid Mech.* **255**, 647–665.

Hagerty, W. W. & Shea, J. F. 1955 A study of the stability of plane fluid sheets. *J. Appl. Mech.* **22**, 509–514.

Huerre, P. & Monkewitz, P. A. 1990 Local and global instabilities in spatially developing flows. *Ann. Rev. Fluid Mech.* **22**, 473–537.

Le Dizès, S. 1997 Global modes in falling capillary jets. *Eur. J. Mech.* B/*Fluids* **16**, 761–778.

Lee, S. L. 1963 Taylor instability of a liquid film around a long, horizontal, circular cylindrical body in still air. *Trans. ASME* E: *J. Appl. Mech.* **85**, 443–447.

Li, X. & Tankin, R. S. 1991 On the temporal instability of a two-dimensional viscous liquid sheet. *J. Fluid Mech.* **226**, 425–443.

Limat, L., Jenffer, P., Dagens, B., Touron, E., Fermigier, M. & Westfreid, J. E. 1992 Gravitational instabilities of thin liquid layers: dynamics of pattern selection. *Physica* D **61**, 166–182.

Lin, S. P. 1981 Stability of a viscous liquid curtain. *J. Fluid Mech.* **104**, 111–118.

Lin, S. P. & Lian, Z. W. 1989 Absolute instability of a liquid jet in a gas. *Phys. Fluids* A **1**, 490–493.

Lin, S. P., Lian, Z. W. & Creighton, B. J. 1990 Absolute and convective instability of a liquid sheet. *J. Fluid Mech.* **220**, 673–689.

Lin, S. P. & Roberts, G. 1981 Waves in a viscous liquid curtain. *J. Fluid Mech.* **112**, 443–458.

Luca, L. de & Costa, M. 1995 Two-dimensional flow of a liquid sheet under gravity. *Computers Fluids* **24**, 401–414.

Luca, L. de & Costa, M. 1997*a* Stationary waves on plane liquid sheets falling vertically. *Eur. J. Mech.* B/*Fluids* **16**, 75–88.

Luca, L. de & Costa, M. 1997*b* Instability of a spatially developing liquid sheet. *J. Fluid Mech.* **331**, 127–144.

Luca, L. de & Meola, C. 1995 Surfactant effects on the dynamics of a thin liquid sheet. *J. Fluid Mech.* **300**, 71–85.

Mathis, C., Provansal, M. & Boyer, L. 1984 The Bénard-Von Karman instability: an experimental study near the threshold. *J. Phys.* (*Paris*) *Lett.* **45**, 483–491.

Monkewitz, P. A. 1988 The absolute and convective nature of instability in two-dimensional wakes at low Reynolds numbers. *Phys. Fluids* **31**, 999–1006.

Monkewitz, P. A. 1990 The role of absolute and convective instability in predicting the behavior of fluid systems. *Eur. J. Mech.* B/*Fluids* **9**, 395–413.

Monkewitz, P. A., Huerre, P. & Chomaz, J. M. 1993 Global linear stability analysis of weakly non-parallel shear flows. *J. Fluid Mech.* **251**, 1–20.

Pritchard, W. G. 1986 Instability and chaotic behaviour in a free-surface flow. *J. Fluid Mech.* **165**, 1–60.

Söderberg, L. D. & Alfredsson, P. H. 1998 Experimental and theoretical stability investigations of plane liquid jets. *Eur. J. Mech.* B/*Fluids* **17**, 689–737.

Squire, H. B. 1953 Investigation of the instability of a moving liquid film. *Brit. J. Appl. Phys.* **4**, 167–169.

Taylor, G. I. 1950 The dynamics of thin sheets of fluid – III. Disintegration of fluid sheets. *Proc. R. Soc. Lond.* A **253**, 313–321.

Teng, C. H., Lin, S. P. & Chen, J. N. 1997 Absolute and convective instability of a viscous liquid curtain in a viscous gas. *J. Fluid Mech.* **332**, 105–120.

Yakubenko, P. A. 1997 Global capillary instability of an inclined jet. *J. Fluid Mech.* **346**, 181–200.